



of using realistic stress conditions and influent geochemistry during hydraulic testing is also demonstrated.

## 1 Introduction

Clay or other low permeability sediment and rock often dominate sedimentary sequences and can form important hydraulic barriers known as aquitards (Potter et al., 1980). Aquitards often overlie aquifers that yield strategically important fresh water resources, and form important cap-rocks or seals between shallow aquifers and deeper strata that are targeted for depressurization during gas or mineral extraction (Timms et al., 2012). The current work compares the results of steady state centrifuge permeability testing of semi-consolidated drill core samples with column tests at standard gravity ( $1g$  at earth's surface,  $9.8065 \text{ (ms}^{-2}\text{)}$ ) and formation scale permeability, based on analysis of in situ pore pressure propagation.

Thick, low  $K$ , unoxidized, clay-rich aquitards represent important sites for waste confinement and disposal (including high-level radioactive waste and sequestration of carbon dioxide and saline effluents) and act as protective covers for regional aquifers (Cherry et al., 2004). Effective shale and claystone flow barriers are required to disconnect shallow aquifer systems from underlying coal seams that are depressurized to produce gas (Timms et al., 2012; APLNG, 2013). Furthermore, fine-grained geologic media are commonly used as engineered barriers to limit horizontal seepage of mine water (Timms et al., 2013), for containment of tailings (Znidarčić et al., 2011) and municipal refuse and nuclear waste (Rowe et al., 1995). Low permeability material is defined by Neuzil (1986) as  $K < 10^{-8} \text{ ms}^{-1}$ . The US EPA requires low permeability waste barriers for hazardous waste landfills with  $K$  of  $< 10^{-9} \text{ ms}^{-1}$  (US EPA, 1989). Neuzil (1986) noted that no geologic material properly tested proved to be entirely impermeable.

Aquitards volumetrically constitute the bulk of sedimentary geologic deposits (Potter et al., 1980), and are typically assumed saturated if located below a watertable

3157

(Cherry et al., 2004). Water-saturated hydraulic conductivity ( $K$ ) and diffusion coefficients for aquitards may therefore not be applicable to variably saturated or non-water saturated low permeability strata. Research on aquitards comprised of semi-consolidated clayey materials deposited by alluvial, colluvial and aeolian processes is lacking, compared with aquitard research on glacial tills (Grisak and Cherry, 1975), claystones (Smith et al., 2013; Jougnot et al., 2010) and shale (Neuzil, 1994; Josh et al., 2012). Clay-bearing sediments formed via alluvial, colluvial and aeolian processes frequently occur in the geosphere. For example, clayey silt aquitards account for 60% of the  $\sim 100 \text{ m}$  thick alluvial sediment sequences, in the Mooki catchment of Australia's Murray–Darling Basin (Farley, 2011) this represents a key gap in the current theoretical understanding of clay mineralogy and geochemistry.

Aquitard research on alluvial sediments is important because recharge by slow seepage provides essential groundwater supplies for municipal water supply and crop irrigation in relatively dry inland settings (Acworth and Timms, 2009). Increased effective stress associated with aquifer drawdown for irrigation, may release saline water stored within shallow aquitards with implications for continuing high yields of fresh water. Characterising the effects of variable chemical composition of formation water on the hydraulic conductivity of such sediments is therefore essential to determine the long-term hydro-geochemical fate of such field sites.

Obtaining realistic measurements of groundwater flow and solute transport within aquitards is by definition a slow process, requiring relatively time consuming and expensive field and laboratory studies. Various field and laboratory methods are available to directly measure or indirectly calculate hydraulic conductivity in a horizontal ( $K_h$ ) or vertical ( $K_v$ ) orientation, and for saturated and semi-saturated or multi-phase flow (e.g. liquid and gas). Water level recovery of a bore pump test in glacial till ( $K = 10^{-11} \text{ ms}^{-1}$ ) for example has occurred over a period of  $\sim 30$  years, with revised calculation of hydraulic parameters to improve the fit with data that is emerging over this time (van der Kamp, 2011).

3158

Methods for measuring the in situ permeability of clay formations include: slug tests (piezometer tests, falling-head tests), aquifer pumping tests with piezometers in the aquitard, aquifer pumping tests with observation wells in the aquifer only, measurement of seasonal fluctuations of pore-pressure, measurement of pore-pressure changes and settlement due to surface loading, and numerical analysis of local and regional groundwater flow (van der Kamp, 2001). Neuman and Witherspoon (1968) developed generic analytical solutions for drawdown within an aquiclude, in which vertical flow occurs, but is sufficient small to have no effect on water levels within an overlying or underlying aquifer. Type curves were presented for analytical solutions applying for an infinitely thick and a finite thickness aquiclude. In contrast, analysis of a leaky aquitard-aquifer system was presented by Neuman and Witherspoon (1972). The ratio method, as it is known, compared drawdown within an aquitard to drawdown in an underlying aquifer from which extraction was occurring. Vertical hydraulic conductivity is calculated from the hydraulic diffusion of pressure transients within a uniform, homogeneous aquitard.

The deconvolution of the pressure response with depth through an aquitard can be analysed with a Fourier transform method known as harmonic analysis (Boldt-Leppin and Hendry, 2003). The hydraulic diffusivity (hydraulic conductivity/specific storage) is expressed analytically either based on the amplitude or phase shift of harmonic signals, assuming that the thickness of the aquitard is half infinite. For example, harmonic analysis enabled in situ  $K_v$  to be estimated from phase and amplitude shifts of pore pressure response to soil moisture loading propagating downwards through a 30 m thick aquitard on the basis of measured specific storage and hourly or 6 hourly groundwater level monitoring over 5 years (Timms and Acworth, 2005). Jiang et al. (2013) further developed the harmonic analysis method for finite aquitards in a multi-layer system, for the case of water level monitoring that is limited to aquifers bounding the aquitard, rather than from within the aquitard. Coherence analysis of water level fluctuations in bounding aquifers from indeterminate stresses (e.g. pumping, recharge, rainfall or earthquake) was used to derive  $K_v$  for deep rock aquitards on the basis of interpolated

3159

groundwater level data that was measured at irregular intervals of at least 10 days for several decades.

A more direct method of determining in situ hydraulic parameters is possible using fully grouted vibrating wire transducers and high frequency data recording within deep formations, as recently demonstrated by Smith et al. (2013) for a bedrock claystone at up to 325 m.b.g.l. (below ground level). Pore pressure and barometric pressure were recorded at 30 min intervals and analysed for barometric response, earth tides, and rainfall events. Core samples from the same drill holes were vacuum sealed on site for consolidation testing and triaxial permeameter testing. The in situ compressibility and specific storage derived from barometric pressure responses were as much as an order of magnitude smaller than laboratory results.

A variety of laboratory testing techniques for low  $K$  samples are also available, however, the reliability of results may depend on factors such as the preparation and size of core samples, configuration of equipment and uncertainties of measurement, the influent water that is used and the stresses that are applied relative to in situ values, and whether permeability is directly measured from steady state flow, or subject to additional parameters and assumptions with alternative flow regime. Laboratory testing of clayey-silt cores by standard rigid and flexible wall column techniques require 1–2 weeks, compared with < 1 week in a centrifuge permeameter methods for unsaturated samples (ASTM, 2010). Constant or falling-head tests in rigid-walled column permeameters at natural gravity require a large water pressure gradient and/or long testing times for low-permeability samples, are subject to potential leakage, and may not replicate in situ confining stresses. Column testing of core samples is possible for some test conditions in triaxial cells such as those used in geotechnical and petroleum studies, such as the study of Wright et al. (2002) on both  $K_h$  and  $K_v$  and anisotropy in limestone aquifers. However, standard practice for testing ultralow permeability cores (e.g.  $K_v < 1 \times 10^{-10} \text{ ms}^{-1}$ ) typically consists of applying a confining pressure to a water tight system and measuring relatively subtle changes in pressure with high resolution pressure transducers (API, 1998).

3160





Selected examples of the various types of hydraulic characterisation tests are provided in Table 1, with further information on the history and development of centrifuge permeameters for these various testing regimes are provided in Sects. 2.4 and 2.5. In contrast to this study of saturated  $K$ , no flow and/or transient types of centrifuge tests are used to determine semi-saturated hydraulic parameters. For example, Nakajima and Stadler (2006) used a 2 m radius centrifuge operating at multiple  $g$ -levels up to  $40g$  for outflow tests to define hydraulic parameters of the van Genuchten model for fluid flow as a function of variable moisture content. This study on fine Ottawa sand samples were tested in a cell of larger dimensions (102 mm diameter and up to 432 mm in height, base of sample at a radius of 1.85 m) and transient fluid pressure data, recorded at points along the sample length, were analysed by inverse modelling to resolve optimum hydraulic parameters.

A centrifuge permeameter, or column mounted on a centrifuge strong box, is commonly used for hydraulic characterisation. A conceptual plan of a centrifuge permeameter is shown in Fig. 1. The centrifuge permeameter contains a cylindrical clay sample with length  $L$  and diameter  $D$ , and is spinning in a centrifuge around a central axis at an angular velocity  $\omega$ . The permeameter has an inlet face at a radius  $r$ , and a drainage plate at a radius of  $r_0$ . The co-ordinate  $z$  is defined as positive from the base of the sample towards the central axis of rotation, consistent with definitions in  $1g$  column testing (McCartney, 2010). This frame of reference is in an opposite direction to that defined by Nimmo and Mello (1991), but is convenient for interpretation and comparison of column flow tests. In this study, the outlet face is a free drainage boundary as discussed further in Sects. 2.4, 3.2 and 5.4.

## 2.4 History of centrifuge permeameters

Centrifuge permeameter techniques have developed over the past two decades (Nimmo and Mello, 1991; Conca and Wright, 1998; McCartney, 2007; Timms, 2005) to enable fluid flow and contaminant transport studies of aquitard materials that would otherwise not be possible, or studies that would take significantly longer using  $1g$  column

3165

permeameter techniques. Early adaptations of relatively small bench-top centrifuge systems meant that each core could be positioned between fluid filled chambers, with a falling head of ponded fluid above the core and an applied pore pressure at the lower core boundary (Nimmo and Mello, 1991).

The Unsaturated Flow Apparatus (UFA) centrifuge system for saturated and unsaturated flow studies introduces influent through a sealed rotary union, with free drainage at the base of each core (Conca and Wright, 1998; Timms, 2003; Timms et al., 2009). However, the radius of this system (0.087 m effective to mid-core, or 0.117 m to base of core) and relatively fast angular velocity results in significantly different  $g$ -levels and stresses along the length of the core. Furthermore, effective flow measurements are only possible by disassembling the core holder. In comparison, real time monitoring of pore pressure has been proven as successful for larger centrifuge systems (McCartney, 2007).

The centrifuge equipment required for faster testing are a disadvantage to widespread adoption, particularly with advanced instrumentation and data transfer challenges within an accelerated gravity environment. Large geotechnical centrifuges (2 to 10 m diameter) are costly to operate and require significant setup time and expertise, whereas the UFA centrifuge is efficient to operate though limited in sample size and the lack of space available to fit instrumentation on the beam for real time data collection (Timms et al., 2003, 2009).

## 2.5 NCGRT Broadbent centrifuge permeameter system

The centrifuge in this study (Fig. 2) is a Broadbent GT-18 Modular Geotechnical Centrifuge (22 kW motor drives a variable speed of 10 to 875 RPM) on which two modules can be fitted: either a centrifuge permeameter GMP GT2/0.65F or a geotechnical beam GMB GT6/0.75F. The geotechnical beam module is not discussed further in this study. The centrifuge permeameter (CP) module was designed specifically for groundwater research while the base centrifuge and geotechnical beam module are standard. Table 2 describes the specifications and performance details of the centrifuge system

3166









Sediments at the Breeza farm and Norman's Road site are relatively heterogeneous, with mixed sandy, clayey sand, and clayey-silt alluvium overlying a semi-confined aquifer. The saturated zone is approximately 18 to 20 m below surface and extraction for flood irrigation of crops causes large fluctuations in groundwater levels in the confined aquifers at > 50 m depth. Hydrogeological and hydrochemical evidence indicate a leaky aquifer-aquitard system (Acworth and Timms, 2009), with the variability in groundwater level responses controlled by a fining upward alluvial sequence (Guinea et al., 2014). At the Norman's Road site, highly saline porewater in the clayey silt near the surface appear to have leached into the underlying aquifer, causing a significant increase in salinity of the aquifer (Badenhop and Timms, 2012).

## 4.2 Drilling and core sampling

Equipment and procedures for coring were compliant with AS 1289.1.1.3 to obtain samples as undisturbed as possible. A rotary drilling rig equipped with Triefus triple core barrels, lined with seamless clear PET, was used in push coring mode. Local creek water was used as a drilling fluid and casing was used to stabilise the hole behind the push core barrel such that drilling fluid additives were not required. The holes were therefore fully cased to the maximum depth of push core drilling at up to 40 mb.g.l.

The non-rotating core barrel was forced into the formation whilst a rotating device on the outside of the tube removes the cuttings as the barrel was advanced. The cutting edge of the non-rotating sample tube projects several millimetres beyond the rotary cutters. The thin walled core barrel complied with the standard for undisturbed sampling, with an area ratio of less than 25 % prescribed by AS 1289.1.1.3 for an open drive sampler. The area ratio of 16 % was based on a core barrel design with an external diameter of 110 mm and internal diameter of 101 mm (C size). The 1.5 m length core barrel was a composite open sampling system with a core nose screwed on the base that included a bevelled end to cut the core as the barrel was pushed into the formation. After the core was extracted from the ground, an air supply was connected

3173

to the top of the core barrel to slide the core out of the barrel whilst retained in the clear PET liner without rotation, distortion or compression.

The cores contained within PET liners in this minimally disturbed state were transferred directly from the core barrels to a cool room on site, and thence to a laboratory cool room, reducing the potential for moisture loss. Semi-consolidated clay cores were selected from below the saturated zone for CP tests, at depths up to 40 mb.g.l. Sediment core samples of lengths between 50–100 mm were prepared for CP testing.

The preferred method for preservation of drill core was double plastic bagging of core sections using a food vacuum sealer, and storage in a cool room at approximately 4 °C. Alternatively, core within PET core barrel liners were trimmed of air or fluid filled excess liner immediately after drilling, sealed with plastic tape, and stored in a cool room. Sections of cores, particularly at the nose end, that appeared to be damaged or disturbed were excluded from permeability or bulk density testing.

After coring, the holes were completed as monitoring piezometers and the casing was jacked out. The piezometers were constructed of screwed sections of 50 mm PVC casing with O-ring seals, with a 1.5 m machine slotted screen packed with pea-sized washed gravel. The annulus was then filled with a bentonite seal, backfilled to the surface and completed with a steel casing monument and cement monument pad.

## 4.3 Groundwater sampling for influent

Fluid for permeability testing (influent) should be taken from the formation at the same depth as the core, or if the limitations of sampling from aquitard strata preclude this, influent water chemistry can be synthesized to approximate known ionic strength, Na/Ca ratio and pH of formation porewater. In this study, groundwater from piezometers at a similar depth to the core was obtained using standard groundwater quality sampling techniques (Sundaram et al., 2009). A 240 V electric submersible pump (GRUNDFOS MP1) and a surface flow cell were used to obtain representative samples after purging stagnant water to achieve constant field measurements of electrical conductivity and other parameters (unpublished data).

3174



A vacuum plate system for core samples was designed and used for two purposes: maximising the moisture content of samples and testing for rapid leaks of core samples that were prepared in acrylic liners in preparation for CP testing. The vacuum plate device was designed to fit the CP liners containing the cores, drawing ponded influent from the top to the base of the cores using a standard laboratory vacuum pump at 1 bar of negative pressure. After 12 to 48 h, or upon effluent flow from the base, the acrylic liners containing the prepared cores were then transferred directly to the CP module without disturbing the sample. Furthermore, the moisture content and degree of saturation was monitoring by weight change of the permeameters during testing, and direct moisture tests of samples before and after CP testing.

#### 5.4 Centrifuge permeameter flow systems and instrumentation

In addition to the Broadbent CP module, some unique systems were developed as part of this study. Influent was fed from a pair of burettes located next to the centrifuge via a pair of custom designed low voltage peristaltic pumps mounted either on the centrifuge beam, or outside the centrifuge and through the low flow rotary union described in Sect. 2.5. The peristaltic pumps can be operated either as zero/maximum flow to a set level, or at a variable flow rate of  $0.001\text{--}150\text{ mL h}^{-1}$ . Manual burette measurements to a resolution of 0.1 mL were used to verify the pump rates.

A PC with LABVIEW software is used for data logging and control of the influent pumping system, originally connected via an Ethernet Optic Rotary Joint (FORJ) that was subsequently replaced by a wireless system. A new data acquisition module (DAS) was designed and constructed with 7 data channels per module, including for influent level monitoring, pressure/load and temperature. A Zigbee based wireless hub was fixed on the centrifuge beam for data transfer from the acquisition modules to a Zigbee wireless modem outside the centrifuge. Low voltage power to the DAS is transferred to the centrifuge beam via slip rings described by Broadbent (2011).

Each permeameter assembly includes a newly designed reservoir insert (see Fig. 4a and b) and employs a pair of custom designed carbon fibre rod electrical conductivity

3177

(EC) electrodes to detect the influent reservoir head to an accuracy of 0.1 mm. The head of influent on the core is typically set to maintain a constant head of influent 20 to 100 mm above the core sample by selection of electrodes of specific length and is therefore maintained at a constant head during *K* testing. The electrodes protrude through a pluviator cap into the influent reservoir and when the reservoir is depleted a decrease in EC is detected and transmitted back to the PC. The corresponding peristaltic pump is then switched on to automatically pump fluid back into the reservoir. Carbon fibre rod (1 mm diameter) was selected as the electrode material due to its high tensile strength, low mass, high electrical conductivity and its resistance to corrosion.

The permeameter is also equipped with effluent reservoir capacity which is connected to the sample via a drainage plate. In order to allow homogenous flow of fluid from the sample surface into the effluent reservoir the drainage plate is lined with one 1 mm thick A14 Geofabrics Bidim geofabric filter (110 micron, and permeability of  $33\text{ ms}^{-1}$ ; AS3706.9-01; Geofabrics, 2009) and one Whatman 5 Qualitative filter paper. The hydraulic conductivity of the drainage plate through a drainage hole of 2 mm diameter was independently measured to ensure that there was no impedance to free drainage. The average permeability > 10 tests of the drainage plate was  $\sim 10^{-5}\text{ ms}^{-1}$  (unpublished data), which is typically a factor of 1000 higher than low permeability core samples.

Effluent is extracted via a syringe or peristaltic pump through a “U” shaped tube that connects to the base of the effluent reservoir (Fig. 4b). The concave dish base of the effluent reservoir has a volume of  $\sim 30\text{ mL}$ . This system, designed by UNSW specifically for these studies, enables samples to be extracted without the need for the permeameters to be taken off the beam, thereby alleviating safety risks in lifting heavy permeameters, and reduces the stop time required for a sampling event during centrifuge flight to less than 5 min.

An air vent, located at the top of the reservoir near the lower end of the drainage plate, connects the reservoir to the outside of the permeameter, thereby maintaining

3178

a zero pressure outflow boundary. The free drainage boundary condition is different from other centrifuge flow setups and is important for subsequent interpretation of flow processes during.

## 5.5 Centrifuge permeameter test operation

- The  $K$  value is based on flow rate, flow area, radius and RPM, although the method was adapted from a UFA centrifuge to this CP system (Sect. 3.2). Importantly, both testing systems are for steady state flow with free drainage due to zero pressure at the base of the core.

Two core samples were balanced to the nearest  $100g$  and tested simultaneously at either end of the centrifuge beam. The centrifuge permeameter was operated at  $10g$  for  $20$ – $30$  min, and if no rapid flows due to leakage were detected, is gradually increased to  $20g$ ,  $40g$  and so on, until the maximum total stress on the core approaches the estimated in situ stresses of the material at its the depth in the formation from which it was cored. It is also important to ensure that effective stress (Sect. 3.3) remains acceptable, as dynamic fluid pressures during testing could cause consolidation of the core matrix, as discussed in Sect. 6.7. Influent volume was measured using both a calibrated continuous time record of pump rotations, and manual burette measurements, and compared to effluent volume until a steady state flow of  $\pm 10\%$  change between measurements was achieved. Section 6.6 discusses the uncertainty of the measured data in more detail.

## 6 Results and discussion

### 6.1 Core index properties

Index properties for five representative cores are provided in Table 3, indicating that these cores were typically silty clay, confirmed by the  $D_{50}$  values of  $< 0.002$  mm that differentiates clay from silt, except for the sandy clay core. The dominance of silty over

clay is an important characteristic of this formation, with clay mineralogy dominated by smectite (Timms and Acworth, 2005; Acworth and Timms, 2009).

- Moisture content varied from  $24.7$  to  $36.4\%$  by weight, and was consistent with site measured data on the core (unpublished data), although not all the cores were fully saturated as received by the external laboratory. Bulk density varied from  $1.71$  to  $1.88 \text{ g cm}^{-3}$  and particle density from  $2.47$  to  $2.58 \text{ g cm}^{-3}$ .

### 6.2 Centrifuge permeameter and $1g$ column tests of cores

The  $K_v$  of cores tested in the CP module (Table 4) varied from  $3.5 \times 10^{-7}$  to  $1.0 \times 10^{-9} \text{ ms}^{-1}$  ( $n = 14$ ). These results were generally higher than  $K_v$  results of  $2 \times 10^{-9}$  to  $4.9 \times 10^{-11} \text{ ms}^{-1}$  ( $n = 7$ ), using column tests (Table 5) at  $1g$ . Accelerations up to  $80g$  were applied during CP testing of semi-consolidated sediment cores and were more typically limited to  $30$ – $40g$ , with test times up to five times faster than by column tests at  $1g$ . The possible reasons for the higher  $K$  results and reduced testing time for CP testing compared with  $1g$  column tests are considered in this section.

- Figure 5 shows the measured influent and effluent rates during a typical CP test as the  $g$ -level is gradually increased, and the calculated  $K_v$  values. The  $g$ -levels were gradually stepped upwards to allow time for excess pore fluid pressures to equilibrate through the core in a sequence that was designed to verify flow rate variability ( $10$ ,  $20$ ,  $40$ ,  $60$ ,  $80$  and back to  $60g$ ). Steady state flow (influent rate equal to effluent rate with no significant change over time) was achieved at  $\sim 20$  h, with some anomalous data earlier in the test (Fig. 5). However, a lower  $K_v$  value was observed over  $> 12$  h overnight, then values measured over  $\sim 1$  h intervals during the day with frequent stops of several minutes duration to measure the effluent volume, the later time interval measurement considered to be more realistic. Further experimentation and numerical modelling is required to adequately explain this discrepancy with may be associated with evaporative losses over longer time periods of flow measurement or other transient processes within the system.

Anomalous flow via preferential pathways could be readily identified by a flow rate several orders of magnitude greater than otherwise observed. Anomalous flow was often observed along the interface of the cores and the liner during the early minutes of a test as sealing occurred at steady state conditions were established. On one occasion, a failure occurred in the core during testing, with a preferential flow path occurring through the matrix, which at accelerated gravity causes very fast flow that is easily detected.

$K_v$  values for cores from the NR and BF sites were significantly more variable (over  $10^{-9}$  to  $10^{-7}$   $\text{ms}^{-1}$ ) than for the CL site (within  $10^{-9}$   $\text{ms}^{-1}$ ). These findings reflect the greater heterogeneity of alluvial sediments at the northern sites (NR and BF), compared with the clayey-silt deposit at the southern CL site. Based on the dataset currently available for each site, there did not appear to be any significant  $K_v$  trend with depth, except at the CL site, with a possible decrease of  $K_v$  by a factor of 3 with depth increasing from 11 to 28 mb.g.l. Further testing is in progress to better identify any spatially significant trends in  $K_v$ .

$K_v$  results obtained from the same CP from these three sites were generally higher than  $K_v$  results from another alluvial system in the western Murray–Darling Basin (unpublished data), and significantly higher than  $K_v$  for consolidated rock cores tested in this system (Bouzalakos et al., 2013). At an undisclosed site in the western Murray–Darling Basin, the hydraulic conductivity of twelve (12) drill cores ranged from  $1 \times 10^{-11}$  to  $6 \times 10^{-6}$   $\text{ms}^{-1}$ , while five (5) cores were  $\leq 10^{-12}$   $\text{ms}^{-1}$  (unpublished data). The relatively low  $g$ -levels, compared to rock core testing (Bouzalakos et al., 2013), were necessary for the shallow and semi-consolidated nature of the clayey-silt cores. In fact, steady state flow was achieved at low  $g$ -levels for  $K_v$  values that were at least 100 times higher than the current detection limit of the CP system.

The uncertainty of reporting results to two significant digits for  $K_v$ , as low as  $10^{-9}$   $\text{ms}^{-1}$  is further discussed in Sect. 6.6. In contrast,  $K_v$  results from an independent laboratory were reported to 3 significant digits for the first batch of samples tested, and

3181

1 significant digits for a subsequent batch of samples, although the range of  $K_v$  values were similar for both batches.

The reduced test times of CP testing may be attributed to the reduced time required to achieve steady state flow with centrifugal forces driving flow. Alternatively, the time required for  $1g$  column testing may have increased due to fluid-solid interactions that reduced infiltration rates into the cores (10 to 100 lower  $K_v$  result for  $1g$  column tests compared with CP tests). It is known that decreased ionic strength of influent (e.g. deionized water) causes a linear decrease in permeability, and that the relative concentrations of sodium and calcium can affect permeability due to swelling and inter-layer interactions (e.g. Shackelford et al., 2010; Ahn and Jo, 2009). It is also possible that differences in  $K$  values from laboratory testing methods can also be attributed to differences in test setup and stress changes that occur as discussed in Sect. 6.7. The centrifuge permeameter uses a larger core size (100 mm diameter) and groundwater sampled near the depth of the core, whereas the  $1g$  column uses a small core diameter (45 mm diameter) and deionized water as an influent.

CP testing was relatively rapid, with an average of less than 16 h (2 to 24 h) required for steady state flow CP, compared with an average of 79 h (48 to 100 h) for  $1g$  column testing. In addition, an extended test of 830 h in the CP (unpublished data) verified that no significant changes occurred over extended testing periods. The CP technique can therefore reduce average testing time to  $\sim 20\%$  of the time that would be required in  $1g$  laboratory testing systems, similar to the reduced time requirement of centrifuge methods for unsaturated hydraulic conductivity functions compared with  $1g$  column tests ASTM (2010). The relative time advantage of testing cores at accelerated gravity may be greater at lower  $K_v$ , due to the increased time required to establish steady state flow conditions. This could be advantageous for longer experiments of contaminant transport that requires several pore volumes of steady state flow.

3182

### 6.3 Validation of results with in situ $K_v$ estimates

There is a general lack of in situ  $K_v$  measurements in this groundwater system. There have been no reported aquifer pump tests in the alluvial aquifer in this area, other than observations of the effects of irrigation bores over various spatial and temporal scales.

5 Vertical hydraulic conductivity ( $K_v$ ) of the clayey-silt at the Cattle Lane site derived from observed amplitude and phase changes, resulted in an average value of  $2.8 \times 10^{-9} \text{ ms}^{-1}$  (Timms and Acworth, 2005). Five major rainfall events occurred during detailed pore pressure monitoring in five piezometers on an hourly or 6 hourly basis over four years. These data were verified and augmented by manual groundwater level  
10 measurements. The phase lag at the base of the clay varied between 49 and 72 days. The phase lag pore pressure analysis resulted in a  $K_v$  value of  $1.6 \times 10^{-9} \text{ ms}^{-1}$ , while the change in amplitude over a vertical clay sequence of 18 m (from a 17 m depth piezometer to the inferred base of the aquitard at 35 m depth) resulted in a  $K_v$  value of  $4.0 \times 10^{-9} \text{ ms}^{-1}$ . The average value of  $K_v$  from these two estimates is  $2.8 \times 10^{-9} \text{ ms}^{-1}$   
15 which is possibly indicative at formation scale in this area, given the thick and extensive lateral extent as discussed below.

The reliability of harmonic analysis related methods may be compromised by specific storage measurements. Jiang et al. (2013) relied on indirect specific storage values derived from downhole sonic and density log data from boreholes in the region, while  
20 Timms and Acworth (2005) calculated specific storage from barometric and loading responses that were recorded in the same groundwater level data set and boreholes that were used for harmonic analysis.

With the advantage of robust estimates for specific storage in this study, the similarity of  $K_v$  measurements different scales at the CL site (Fig. 6) indicates that in this  
25 part of the alluvial deposit,  $K$  is independent of the scale of measurement and that no hydraulically active fractures or vertical flowpaths affected the data. As discussed further in Sect. 6.8, this finding is consistent with work on argillaceous strata by Neuzil

3183

(1994), but contrasts with evidence of scale dependant  $K$  values in other groundwater systems.

5 Electrical resistivity tomography (Fig. 7) at the CL site confirmed the lateral extent of the relatively uniform formation in this area of the catchment. An electrical resistivity tomograph model indicated a homogenous layered system over a 240 m extent with resistivity increasing with depth to about 10 m depth, and then is relatively similar to a depth of about 30 m. This confirms a relatively uniform sediment in this area as found by CPT profiling by Wiesner and Acworth (1999).

### 6.4 Comparison of results with regional $K_v$ estimates

10 A regional groundwater flow model developed by McNeilage (2006) with a 2 layer MODFLOW code, determined the dominant source of recharge to be diffuse leakage through the soil (and aquitards) in the Breeza area (Zone 3 groundwater management area). As in typical modelling practice (Barnett et al., 2012), water the aquitard was not explicitly modelled, with water instead transferred from a shallow to a deeper aquifer using  
15 a vertical leakance value (units in  $\text{dy}^{-1}$ ), a model variable that is calculated for each cell of the model.

The calibrated groundwater model indicated that approximately 70 % of the long term average groundwater recharge ( $11 \text{ GL yr}^{-1}$ ) was attributed to diffuse leakage in this area that included the CL and NR sites. This volume is equivalent to  $20 \text{ m yr}^{-1}$ , or  
20 a  $K_v$  of  $\sim 6 \times 10^{-10} \text{ ms}^{-1}$  assuming a unit vertical hydraulic gradient over an area of approximately  $500 \text{ km}^2$ . The actual  $K_v$  or leakance values were not reported. The calibrated leakance values were found to vary over three orders of magnitude across the Breeza area, with relatively high values in isolated area in the south, centre and north. In comparison, the  $K_v$  results on clayey-silt cores appear to be higher, but with a similar  
25 degree of heterogeneity.

3184

## 6.5 Linear flow velocity at natural gradient and accelerated conditions

To determine if accelerated flow conditions are realistic for hydrogeological environments, the linear flow velocity (apparent flow velocity corrected for porosity) for various CP setups was compared with a theoretical unit gradient, and a typical vertical in situ vertical hydraulic gradient. Figure 8 illustrates concepts for fluid flow at accelerated gravity. The hydrostatic fluid pressure (Eq. 9), measured at a radial position within the core sample, increases with distance from the axis of rotation, continuing into a pressured reservoir boundary, or decreasing to zero at a free drainage boundary. By contrast, the centrifuge inertial (elevation) head decreases with increasing distance from the axis of rotation, as also shown by Nimmo and Mello (1991) and McCartney (2007). It follows that the direction of fluid flow is outwards, in the opposite direction to the axis of rotation. The gradients that drive flow are depicted in Fig. 8b, with the most significant driving force due to centrifugal acceleration. The numerical analysis of fluid pressures that develop during flow and transition to new  $g$ -levels is beyond the scope of the current study.

In Table 6, an in situ hydraulic gradient of 0.5 is compared with CP setups for 100 mm and 65 mm diameter cores of various lengths, for an aquitard material with  $K_v$  of  $10^{-8} \text{ ms}^{-1}$ . The vertical flow rate varies from  $0.3 \text{ mL h}^{-1}$  under in situ conditions, to  $8.5 \text{ mL h}^{-1}$  in the CP, such that linear flow velocities remain very low  $10^{-8}$  to  $10^{-6} \text{ ms}^{-1}$ . The flow rate during centrifugation was  $N$  times greater than if a hydraulic gradient of 1 was applied to the core samples at  $1g$ . This increase in flow rate is consistent with scaling laws for physical modelling (Tan and Scott, 1987), and is greater than would occur within aquitards where the vertical hydraulic gradient is typically less than one. An in situ vertical hydraulic gradient determined from measurements in piezometers that are located above, below and within the aquitard sequence can provide hydraulic gradients that are typically higher than hydraulic gradients for lateral flow.

Steady state flow  $K_v$  testing in the CP requires a relatively short testing time, as described in Sect. 6.2, whereas for solute transport experiments, a longer experimental

3185

time is required for several pore volumes (PV) of flow. For example, Timms and Hendry (2008) and Timms et al. (2009) describe continuous CP experiments over 90 days to quantify reactive solute transport. The comparisons of time required for one PV provided in Table 6 illustrate the possible advantages of CP for contaminant flow that may affect the structural integrity of the material.

## 6.6 Limits and uncertainties of centrifuge permeameter testing

$K$  values measured in this study are within the range of applicability of Darcy's Law for laminar flow at accelerated gravity. Flow of fluid through porous media at accelerated gravity was found by Nimmo et al. (1987) to follow Darcy's law for accelerations below  $1600g$ . The low end of  $K$  values that have been measured for geological specimens in the laboratory is  $10^{-16} \text{ ms}^{-1}$  (equivalent to approximately  $10^{-11}$  Darcy, or  $10^{-19} \text{ cm}^2$ ) in the UFA centrifuge (Conca and Wright, 1998). At accelerated gravity, steady state flow equilibrium is achieved in a time of hours and days, and in situ stresses can be applied to drill core from approximately  $< 100 \text{ m}$  depth or a total stress of approximately  $1 \text{ MPa}$  in the Broadbent CP system (without weighting discs).

Hydraulic conductivity data derived from experiments in the centrifuge permeameter include a component of measurement error. The quantified components of the measurement error are: limit of reading for time  $\pm 1 \text{ s}$ ; limit of reading for permeameter (total mass) balance  $\pm 0.5g$ ; limit of reading for high precision (outflow mass) balance  $\pm 0.1g$ ; limit of reading for influent control burette  $\pm 0.1 \text{ mL}$ ; accuracy of automatic influent control system  $\pm 0.1 \text{ mL}$ ; accuracy of influent fluid level monitoring system  $\pm 0.2 \text{ mm}$ ; fluid held by surface tension in effluent reservoir and on reservoir base plate  $< \pm 1.0 \text{ mL}$ ; evaporation from permeameter chambers  $< 0.3 \text{ mm d}^{-1}$  ( $< 2.2 \text{ mL dy}^{-1}$  at  $875 \text{ RPM}$ ).

Sidewall leakage between the core-sample and wall of the permeameter, and any resin that is required to set the core sample for testing has been quantified and is below the hydraulic conductivity detection limit. The current detection limit of the centrifuge permeameter ranges from  $3 \times 10^{-11}$  to  $1 \times 10^{-12} \text{ ms}^{-1}$  and is controlled by evaporation which increases with increasing centripetal acceleration. For the low levels required

3186





parameterising this variability in flow models, predictions of groundwater impacts from aquifer interference activities can exhibit a significant degree of uncertainty. Core scale measurements of aquitard properties provide an opportunity to reduce this uncertainty by providing a likely minimum value of matrix permeability if the cores are drilled, preserved, prepared and tested in an appropriate manner as demonstrated in this study.

For argillaceous strata permeability often does not increase with increasing physical scale of testing at least at intermediate scale, indicating that permeability due to fracturing is absent (Neuzil, 1994). In the absence of direct measurement of aquitard permeability there is a real risk that aquitard parameters may be ignored or misrepresented in analyses resulting in a corresponding under-prediction of vertical connectivity via preferential flow paths and/or over-prediction of aquifer storage and transmissivity. This is an especially important consideration in the analysis of aquifer tests that may not have been conducted for sufficient periods of time to identify distant boundary conditions or the characteristic effects of aquitard leakage and/or storage (Neuman and Witherspoon, 1968). In very low permeability strata however, there are practical limitations to pump tests and packer testing below about  $10^{-8} \text{ ms}^{-1}$ , depending on the equipment and the length of strata that is subject to testing. It is recognised that in many heterogeneous systems that time lags for the propagation of drawdown responses through an aquitard can be significant (Kelly et al., 2013).

Core scale measures of aquitard hydraulic conductivity are an integral component of hydrogeological studies concerning aquifer connectivity. The availability of core scale facies measurements enables the up-scaling of bore log and geophysical data to determine upper and lower hydraulic conductivity bounds for regionally up-scaled aquitard units. Any differences between  $K$  values at various scale is important for indicating the possibility of preferential flow through heterogeneous strata or aquitard defects (e.g. faults and fractures). The availability of these bounded estimates helps to constrain the uncertainty analyses conducted on regional groundwater flow models to yield more confident predictions (Gerber and Howard, 2000).

3189

Nevertheless, aquitards are typically excluded from regional groundwater flow models, which rely on hydraulic resistance (leakance) values to transfer water vertically between aquifers (Barnett et al., 2012). However, such an approach is not capable of identifying rapid flow pathways through defects in the aquitards or the release of stored water from an aquitard to an aquifer and cannot resolve the vertical hydraulic head distribution across the aquitard to verify drawdown responses. An aquitard should be subdivided into at least three thinner layers to effectively model transient pressure responses (Barnett et al., 2012). Rather than assigning constant theoretical values for aquitard properties through these multiple layers, a combination of realistic and rapid laboratory measurement and direct in situ measurements may be considered where high risk activities demand improved confidence in conceptual understanding and model predictions.

## 7 Conclusions and further work

Accurate and reliable measurement of the vertical hydraulic conductivity of aquitards is a critical concern for many applications. More realistic numerical flow models are possible to quantify the significance of transient drawdown, the associated release of water into adjacent aquifers over long time periods, and the possibility of preferential flow. However, increasing the complexity of hydro-geochemical models cannot improve confidence in the conceptual model if the original data on aquitard hydraulic properties is inaccurate or absent.

Centrifuge technology can be a powerful tool for hydraulic and geotechnical characterization of low permeability sediments and rocks to augment site and regional scale assessments. The lengthy time required to obtain realistic aquitard hydraulic data is substantially reduced by achieving hydraulic equilibrium under accelerated gravity. Value can be added to the cost of drilling if strata samples are drilled using coring methods with minimal disturbance, preserving the cores to prevent moisture loss, and appropriate preparation and testing of the cores as demonstrated in this study.

3190

Core tests using formation water or groundwater as an influent with realistic stresses can provide a reliable minimum matrix scale value for evaluating the potential for vertical flow at a larger scale. Any differences between  $K$  values at various scale is important for indicating the possibility of preferential flow through heterogeneous strata or aquitard defects (e.g. faults and fractures).  $K_v$  results in the order of  $10^{-9} \text{ ms}^{-1}$  were obtained in  $\sim 20\%$  of the time required for  $1g$  column permeameter tests. The  $K_v$  values were successfully verified with independent in situ  $K_v$  values calculated from high frequency pressure data changes within a thick, homogenous and laterally extensive clayey-silt deposit. This provides confidence for contaminant transport experiments that require several pore volumes of influent flow at steady state conditions, but would otherwise require implausibly lengthy testing periods without accelerated flow rates.

Further studies are in progress in the CP to measure both  $K_v$  and  $K_h$  to assess the anisotropy of core samples, to quantify the effect of deionized water and varying influent chemistry on  $K_v$ , and to consider the significance of transient fluid pressure and changes in stress regimes during accelerated fluid flow in these porous media. Additional instrumentation to monitor changes in moisture content and fluid pressure/suction within the core is required to examine the effects of desaturation on strata integrity and hydraulic behaviour.

*Acknowledgements.* Funding from the Australian Research Council and National Water Commission, through the National Centre for Groundwater Research and Training Program 1B is gratefully acknowledged. The contributions of N. Baker and A. Ainsworth of Broadbent and Sons, Huddersfield UK, are acknowledged and J. McCartney for helpful discussion on the theory of fluid flow during centrifuge testing. We appreciated research support at the Breeza farm provided by M. McLeod and S. Goodworth of the NSW Department of Primary Industries. Clayey-silt cores were drilled by New South Wales Office of Water, with S. McCulloch, H. Studhome and G. Regmi. Experimental testing was assisted at UNSW by A. Hartland, B. Bambrook, M. Aitkins, P. King, S. May and T. Meyers.

3191

## References

- Acworth, R. I.: Investigation of dryland salinity using the electrical image method, *Aust. J. Soil Res.*, 37, 623–636, 1999.
- Acworth, R. I. and Timms, W.: Evidence for connected water processes through smectite-dominated clays at Breeza, New South Wales, *Aust. J. Earth Sci.*, 56, 71–86, 2009.
- Ahn, H. S. and Young Jo, H. Y.: Influence of exchangeable cations on hydraulic conductivity of compacted bentonite, *Appl. Clay Sci.*, 44, 144–150, 2009.
- Arulanandan, K., Thompson, P. Y., Kutter, B. L., Meegoda, N. J., Muraleetharan, K. K., and Yogachandran, C.: Centrifuge modeling of transport processes for pollutants in soils, *J. Geotech. Eng.-ASCE*, 114, 185–205, 1988.
- API: Recommended Practices for Core Analysis, Recommended Practice 40, 2nd Edn, American Petroleum Institute Publishing Services, Washington, DC, 1998.
- APLNG: Groundwater Assessment, Australia Pacific LNG Upstream Project Phase 1, Q-LNG01-15-TR-1801, Australia Pacific LNG, Milton, Queensland, Australia, 266 pp., 2013.
- AS: Methods of Testing Soil for Engineering Purposes, Standard methods 1289 2.1.1; 5.1.1; 5.3.2 and 6.7.3, Australian Standards, Sydney, 1991.
- AS: Sampling and Preparation of Soils – Undisturbed Samples – Standard Method 1289 1.3.1. Australian Standards, Sydney, 1999.
- ASTM: Standard Test Method for Determining Unsaturated and Saturated Hydraulic Conductivity in Porous Media by Steady State Centrifugation, D 6527-08, American Society for Testing and Materials International, West Conshohocken, PA, United States, 2008.
- ASTM: Standard Test Method for Measurement of Hydraulic Conductivity of Unsaturated Soils, D 7664-10, American Society for Testing and Materials International, West Conshohocken, PA, United States, 2010.
- Badenhop, A. M. and Timms, W. A.: Long-Term Salinity Changes in an Inland Aquifer, NSW, Australia, in: Proceedings of the 34th Hydrology & Water Resources Symposium, Engineers Australia, Sydney, NSW, 43–51, 19–22 November 2012.
- Bambrook, B.: Aquitards and Groundwater Sustainability – Comparison of Geotechnical Centrifuge Tests and Computer Models, Unpublished Honours thesis, School of Civil and Environmental Engineering, University of New South Wales, 2011.

3192

- Barnett, B., Townley, L. R., Post, V., Evans, R. E., Hunt, R. J., Peeters, L., Richardson, S., Werner, A. D., Knapton, A., and Boronkay, A.: Australian Groundwater Modelling Guidelines, published by the National Water Commission, Australia, 2012.
- 5 Boldt-Leppin, B. E. J. and Hendry, J. M.: Application of harmonic analysis of water levels to determine vertical hydraulic conductivities in clay-rich aquitards, *Ground Water*, 41, 514–522, 2003.
- Bouzalakos, S., Timms, W., Rahman, P., McGeeney, D., and Whelan, M.: Geotechnical centrifuge permeater for characterizing the hydraulic integrity of partially saturated confining strata for CSG operations, in: *Reliable Mine Water Technology, Vol. I, Proceedings of the International Mine Water Congress, Colorado School of Mines, 5–9 August 2013*, edited by: Brown, A., Figueroa, L., and Wolkersdorfer, Ch., Publication Printers, Denver, Colorado, USA, 1193–1198, 2013.
- Broadbent: Operating Manual for Modular Geotechnical Centrifuge with GT2/0.65 Permeameter and GT6/0.75 Beam Environments, Broadbent and Sons Ltd., Huddersfield, UK, 2011.
- 10 Cherry, J. A., Parker, B. L., Bradbury, K. R., Eaton, T. T., Gotkowitz, M. G., Hart, D. J., and Borchardt, M. A.: Role of Aquitards in the Protection of Aquifers from Contamination: a “State of the Science” Report, AWWA Research Foundation, Denver, CO, United States, 2004.
- Conca, J. L. and Wright, J.: The UFA method for rapid, direct measurements of unsaturated transport properties in soil, sediment and rock, *Aust. J. Soil Res.*, 36, 1–25, 1998.
- 20 Farley, C.: Aquitards and Groundwater Sustainability: Three-Dimensional Mapping of Aquitard Architecture, Unpublished Honours thesis, School of Civil and Environmental Engineering, University of New South Wales, 2011.
- Garnier, J., Gaudin, C., Springman, S. M., Culligan, P. J., Goodings, D., Konig, D., Kutter, B., Phillips, R., Randolph, M. F., and Thorel, L.: Catalogue of scaling laws and similitude questions in geotechnical centrifuge modelling, *International Journal of Physical Modelling in Geotechnics*, 3, 1–23, 2007.
- Geofabrics: bidim® Technical Data Sheet – Nonwoven Polyester Geotextile, M018 02 09, Geofabrics Australasia Pty Ltd, Melbourne, Australia, 2009.
- Gerber, R. E. and Howard, K.: Recharge through a regional till aquitard: three-dimensional flow model water balance approach, *Ground Water*, 38, 410–422, 2000.
- 30 Grisak, G. E. and Cherry, J. A.: Hydrologic characteristics and response of fractured till and clay confining a shallow aquifer, *Can. Geotech. J.*, 12, 23–43, 1975.
- Head, K. H.: *Manual of Soil Laboratory Testing*, Pentech Press, London, 1988.

- Jiang, Z., Mariethoz, G., Taulis, M., and Cox, M.: Determination of vertical hydraulic conductivity of aquitards in a multilayered leaky system using water-level signals in adjacent aquifers, *J. Hydrol.*, 500, 170–182, 2013.
- 5 Josh, M., Esteban, L., Delle Piane, C., Sarout, J., Dewhurst, D. N., and Clenell, M. B.: Laboratory characterisation of shale properties, *J. Petrol. Sci. Eng.*, 88, 107–124, doi:10.1016/j.petrol.2012.01.023, 2012.
- Jougnot, D., Revil, A., Lu, N., and Wayllace, A.: Transport properties of the Callovo–Oxfordian clay rock under partially saturated conditions, *Water Resour. Res.*, 46, W08514, doi:10.1029/2009WR008552, 2010.
- 10 Kelly, B. F. J., Timms, W. A., Andersen, S. M., Ludowici, K., Blakers, R., Badenhop, A., McCallum, A. M., Rau, G. C., and Acworth, R. I.: Aquifer heterogeneity and response time: the challenge for groundwater management, *Crop Pasture Sci.*, 64, 1141–1154, doi:10.1071/CP13084, 2013.
- Loke, M. H.: *Rapid 2-D and 3-D Resistivity and IP Inversion Using the Least Squares Method – RES2DINV Ver 3.4 Manual*, available at: [www.geoelectrical.com](http://www.geoelectrical.com) (last access: 18 January 2014), 2001.
- 15 McCartney, J. S.: Determination of the Hydraulic Characteristics of Unsaturated Soils Using a Centrifuge Permeameter, Ph.D. thesis, The University of Texas at Austin, Faculty of the Graduate School, 2007.
- 20 McCartney, J. S. and Zornberg, J. G.: Centrifuge permeameter for unsaturated soils II: measurement of the hydraulic characteristics of an unsaturated clay, *J. Geotech. Geoenviron.*, 136, 1064–1076, 2010.
- McNeilage, C.: *Upper Namoi Groundwater Flow Model*, NSW Department of Natural Resources, New South Wales, Parramatta, 2006.
- 25 Nakajima, H. and Stadler, A. T.: Centrifuge modeling of one-step outflow tests for unsaturated parameter estimations, *Hydrol. Earth Syst. Sci.*, 10, 715–729, doi:10.5194/hess-10-715-2006, 2006.
- Neuman, S. P. and Witherspoon, P. A.: Theory of flow in aquicludes adjacent to slightly leaky aquifers, *Water Resour. Res.*, 4, 103–112, 1968.
- 30 Neuman, S. P. and Witherspoon, P. A.: Field determination of the hydraulic properties of leaky multiple aquifer systems, *Water Resour. Res.*, 8, 1284–1298, 1972.
- Neuzil, C. E.: Groundwater flow in low permeability environments, *Water Resour. Res.*, 22, 1163–1195, 1986.

- Neuzil, C. E.: How permeable are clays and shales?, *Water Resour. Res.*, 30, 145–150, 1994.
- Nimmo, J. R. and Mello, K. A.: Centrifugal techniques for measuring saturated hydraulic conductivity, *Water Resour. Res.*, 27, 1263–1269, 1991.
- 5 Nimmo, J. R., Rubin, J., and Hammermeister, D. P.: Unsaturated flow in a centrifugal field: measurement of hydraulic conductivity and testing of Darcy's Law, *Water Resour. Res.*, 23, 124–134, 1987.
- Parks, J., Stewart, M., and McCartney, J. S.: Validation of a centrifuge permeameter for investigation of transient infiltration and drainage flow processes in unsaturated soils, *Geotech. Test. J.*, 35, Paper ID: GTJ103625, doi:10.1520/GTJ103625, 2012.
- 10 Potter, P. E., Maynard, J. B., and Pryor, W. A.: *Sedimentology of Shale – Study Guide and Reference Source*, Springer-Verlag, New York, 1980.
- Rowe, R. K., Quigley, R. M., and Booker, J. R.: *Clayey Barrier Systems for Waste Disposal Facilities*, E & FN Spon, London, 1995.
- Schulze-Makuch, D., Carlson, D. A., Cherkauer, D. S., and Malik, P.: Scale Dependency of hydraulic conductivity in heterogeneous media, *Ground Water*, 37, 904–919, 1999.
- 15 Shackelford, C. D., Sevick, G. W., and Eykholt, G. R.: Hydraulic conductivity of geosynthetic clay liners to tailings impoundment solutions, *Geotext. Geomembranes*, 28, 149–162, 2010.
- Šimůnek, J. and Nimmo, J.: Estimating soil hydraulic parameters from transient flow experiments in a centrifuge using parameter optimization technique, *Water Resour. Res.*, 41, 1–9, 2005.
- 20 Singh, D. N. and Gupta, A. K.: Modelling hydraulic conductivity in a small centrifuge, *Can. Geotech. J.* 37, 1150–1155, 2000.
- Smith, L. A., van der Kamp, G., and Hendry, M. J.: A new technique for obtaining high-resolution pore pressure records in thick claystone aquitards and its use to determine in situ compressibility, *Water Resour. Res.*, 9, 732–743, 2013.
- 25 Sundaram, B., Feitz, A., de Caritat, P., Plazinska, A., Brodie, R., Coram, J., and Ransley, T.: *Groundwater Sampling and Analysis – a Field Guide*, Geoscience Australia, Record 2009/27, 95 pp., 2009.
- Tan, T. S. and Scott, R. F.: Centrifuge scaling considerations for fluid–particle systems: discussion by R. N. Taylor and response, *Geotechnique*, 37, 131–133, 1987.
- 30 Timms, W. and Acworth, R. I.: Propagation of porewater pressure change through thick clay sequences: an example from the Yarramanbah site, Liverpool Plains, New South Wales, *Hydrogeol. J.*, 13, 858–870, doi:10.1007/s10040-005-0436-7, 2005.

3195

- Timms, W. and Acworth, R. I.: Rethinking a Conceptual Model: Advective vs. Diffusive Chloride Flux in a Low Permeability Clay Sequence, *International Association of Hydrogeologists Congress on Aquifer Systems Management*, Dijon, France, 30 May–1 June, 2006.
- 5 Timms, W. A. and Hendry, M. J.: Long term reactive solute transport in an aquitard using a centrifuge model, *Ground Water*, 46, 616–628, doi:10.1111/j.1745-6584.2008.00441.x, 2008.
- Timms, W. A., Hendry, M. J., Sharma, J., and Cooper, C.: Application of centrifuge modelling to assess long-term brine migration in thick clay tills, Saskatchewan, Canada, in: *Proceedings of Water in Mining*, Australian Institute of Mining and Metallurgy (AusIMM), Brisbane, 13–15 October 2003, 2003.
- 10 Timms, W., Hendry, J., Muise, J., and Kerrich, R.: Coupling centrifuge modeling and laser ablation ICP-MS to determine contaminant retardation in clays, *Environ. Sci. Technol.*, 43, 1153–1159, 2009.
- Timms, W., Acworth, I., Hartland, A., and Laurence, D.: Leading practices for assessing the integrity of confining strata: application to mining and coal seam gas extraction, in: *International Water and Mining Association Symposium Proceedings*, Bunbury, Western Australia, 29 September to 4 October 2012, edited by: Clint, D., McCullough, C. D., Lund, M. A., and Wyse, L., 139–148, 2008.
- 15 Timms, W., Whelan, M., Acworth, I., McGeeney, D., Bouzalakos, S., Crane, R., McCartney, J., and Hartland, A.: A novel centrifuge permeameter to characterize flow through low permeability strata, in: *Proceedings of International Congress on Physical Modelling in Geotechnics (ICPMG)*, Perth, Balkema, 14–17 January, 2014.
- US EPA: Requirement for Hazardous Waste Landfill Design, Construction and Closure, EPA/625/4-89/022, US Environmental Protection Agency, Cincinnati, OH, United States, 1989.
- 25 Van der Kamp, G.: Methods for determining the in situ hydraulic conductivity of shallow aquitards – an overview, *J. Hydrol.*, 9, 5–6, 2001.
- Van der Kamp, G.: Determining the hydraulic properties of aquitards, in: *2nd Canadian Symposium on Aquitard Hydrogeology*, University of Ottawa, Canada, 21–23 June, 2011.
- Wiesner, T. and Acworth, R. I.: Groundwater Contamination Investigation Using CCPTs, *Water* 99 Joint Congress, Brisbane, Australia, 6–8 July, 1999.
- 30 Wright, M., Dillon, P., Pavelic, P., Peter, P., and Nefiodovas, A.: Measurement of 3-D hydraulic conductivity in aquifer cores at in situ effective stress, *Ground Water*, 40, 509–517, 2002.

3196





**Table 4.**  $K_v$  results from CP tests indicating  $g$ -level maximum and testing time. The influent source column identifies the site (NR, CL, BF) and depth (P20 is piezometer screen at 20 m depth) of groundwater sampling. Calculations were based on Eq. (9) for  $K_v$  and Eq. (11) for in situ stress.

Site	Test ID	Depth (mb.g.l.)	$K_v$ ( $\text{ms}^{-1}$ )	$g$ -level maximum	Estimated in situ stress (kPa)	Testing time (h)	Influent source
NR	5-1	33.8	$4 \times 10^{-9}$	10	615	~ 144	NR P30
NR	5-2	33.9	$2 \times 10^{-9}$	10	615	~ 144	NR P30
NR	37-1	34.68	$2.4 \times 10^{-7}$	10	646	2.6	NR P30
CL	36-1	11.75	$3.5 \times 10^{-9}$	80	219	24	CL P15
CL	36-2	19.25	$2.0 \times 10^{-9}$	80	359	24	CL P20
CL	39-1	26.01	$2.4 \times 10^{-9}$	80	485	21	CL P40
CL	39-2	26.10	$1.1 \times 10^{-10}$	80	486	21	CL P40
CL	53-1	28.33	$2.0 \times 10^{-9}$	10	526	24	CL P40
BF	34-1	24.07	$5.9 \times 10^{-9}$	40	449	3	BF CP25
BF	34-2	24.14	$3.4 \times 10^{-8}$	40	450	3	BF CP25
BF	53-2	31.4	$1.3 \times 10^{-9}$	30	567	11.1	BF CP40
BF	37-2	36.46	$3.5 \times 10^{-7}$	10	680	2.5	BF CP40
BF	35-1	40	$1.5 \times 10^{-9}$	30	746	23	BF CP40
BF	35-2	40	$4.3 \times 10^{-8}$	30	746	23	BF CP40

3201

**Table 5.** Independent  $1g$  column permeameter results (vertical uniaxial stress 100 kPa, influent was water that was deionized by distillation).

Core Site	Depth (mb.g.l.)	Apparent $K_v$ ( $\text{ms}^{-1}$ )	Testing time (h)
CL	11.27–11.47	$1.4 \times 10^{-9}$	96
CL	11.27–11.47	$1.1 \times 10^{-10}$	73
CL	28.24–28.33	$1.5 \times 10^{-10}$	100

3202



**Table 6.** Linear flow velocity at natural gradient, unit gradient and for various centrifuge permeameter setups.

	Natural gradient	Unit gradient	Centrifuge permeameter		
Vertical hydraulic conductivity ( $\text{ms}^{-1}$ )			$1.0 \times 10^{-8}$		
Core type		C core – long	C core – short	HQ core – short	
Core length $\times$ diameter (mm)		200 $\times$ 100	30 $\times$ 100	30 $\times$ 65	
RPM	n/a	n/a	202	202	310
$g$ -level	1	1	30	30	70
Vertical fluid head gradient ( $\text{m m}^{-1}$ )	0.5	1	$\sim 0.2^*$	$\sim 0.5^*$	$\sim 0.5^*$
Flow ( $\text{mLh}^{-1}$ )	0.3	0.6	8.5	8.5	8.5
Linear flow velocity ( $\text{ms}^{-1}$ )	$1.7 \times 10^{-8}$	$3.3 \times 10^{-8}$	$1.0 \times 10^{-6}$	$1.0 \times 10^{-6}$	$2.4 \times 10^{-6}$
Time for 1 pore volume (h)	3333	1667	55.4	8.3	3.5
			Normalised		
Increased linear flow velocity			30	30	71
Reduced time for 1 PV			30	200	474

\* Fluid head gradient depends on the depth of influent on the core, and the length of the core.

3203

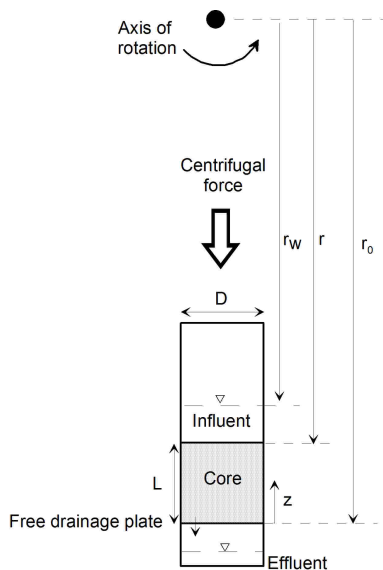


**Fig. 1.** Cross-sectional diagram of a core sample subjected to centrifugal force, with a free drainage boundary condition at the base of the core.

3204

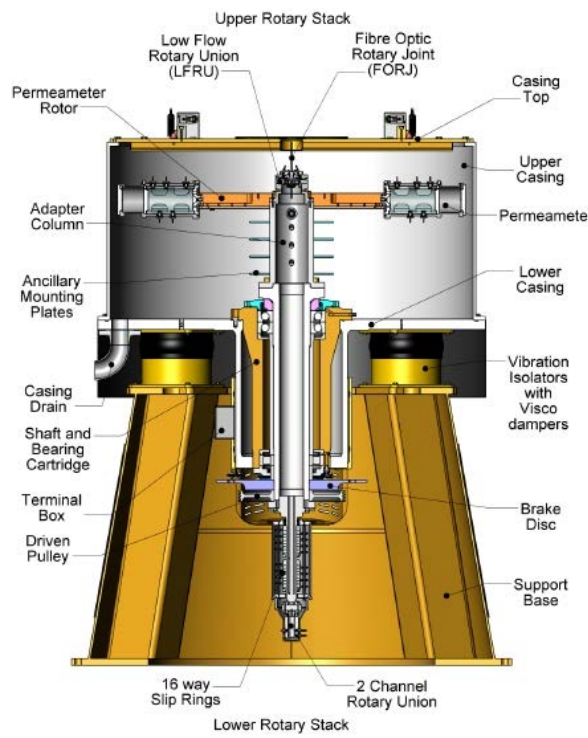


**Fig. 2.** Schematic diagram of the NCGRT geotechnical centrifuge and permeameter module in cross-section (Broadbent, 2011).

3205

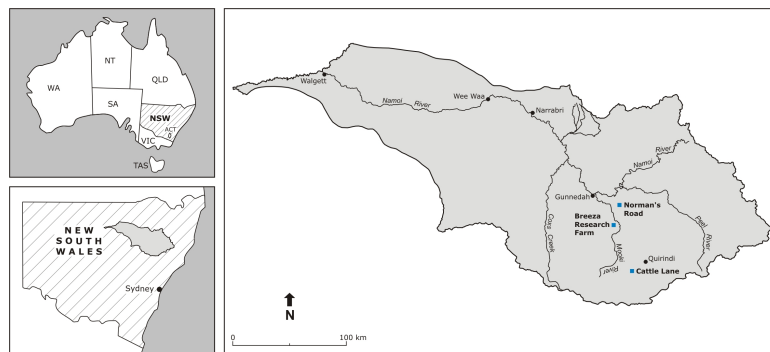


**Fig. 3.** Location of study sites in Eastern Australia, state of NSW. The Norman's Road, Breeza Farm and Cattle Lane sites are shown within the Namoi catchment.

3206

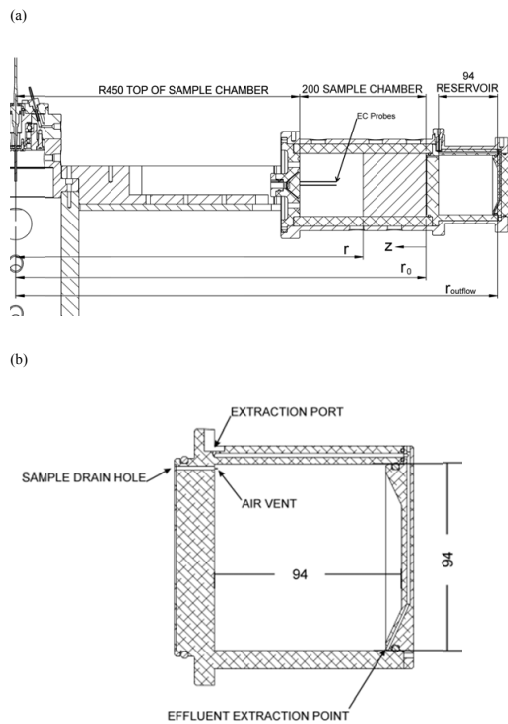


**Fig. 4.** Cross section of the (a) centrifuge permeameter and beam showing new reservoir and reference points and (b) detail of new reservoir liner with suction extraction port.

3207

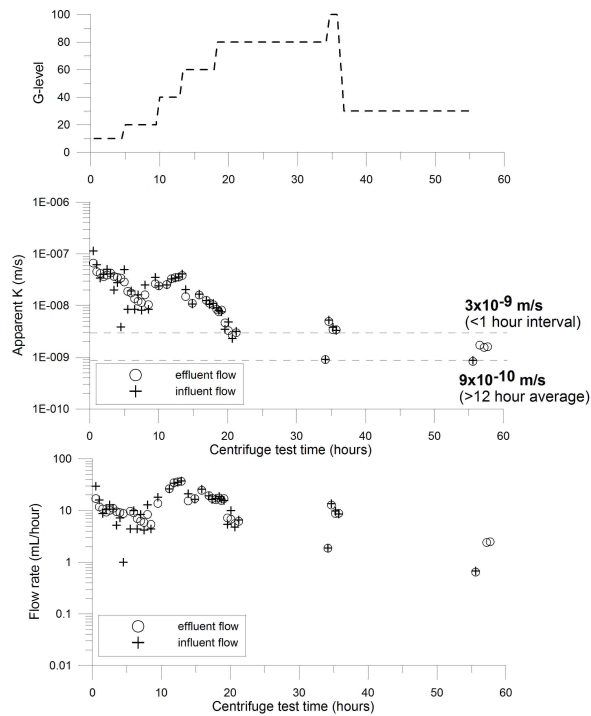


**Fig. 5.** Centrifuge permeameter testing at low stresses of a semi-consolidated clayey-silt core sample (CL 26.1 m depth, Test 39-1) showing variation of  $g$ -level,  $K_v$  and influent and effluent flow rate during the test (after Timms et al., 2014).

3208

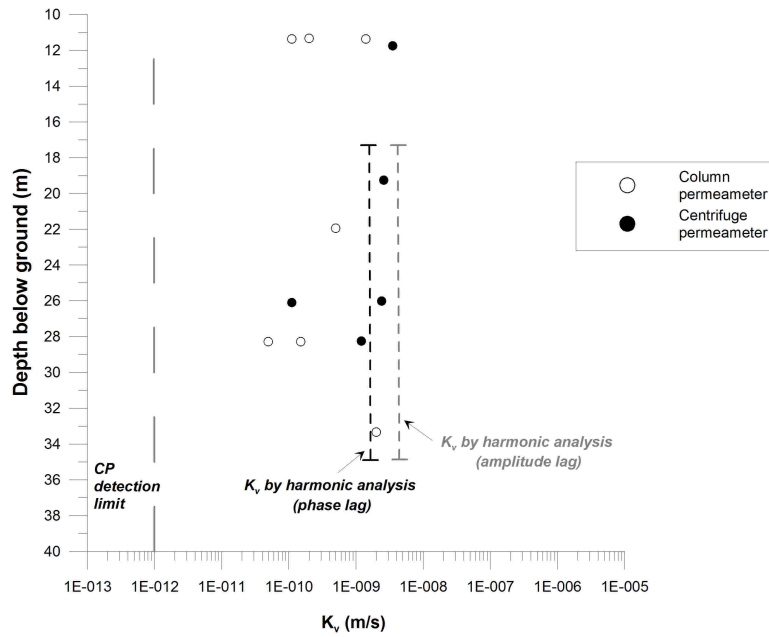


**Fig. 6.** Vertical hydraulic conductivity measurements by centrifuge permeameter, column permeameter. These data are compared with in situ pore pressure data at 6 hourly intervals over 5 years interpreted with harmonic analysis (after Timms and Acworth, 2005) for the Cattle Lane site with massive clayey-silt from the surface to 35 m depth.

3209

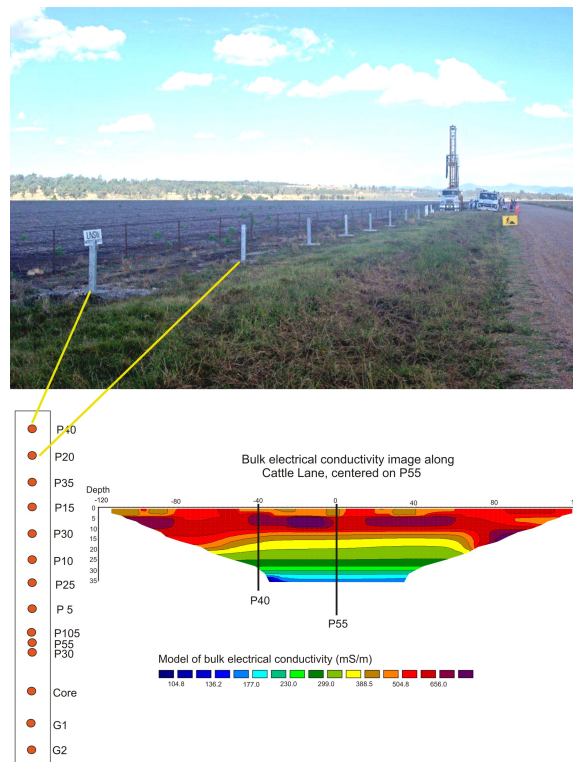


**Fig. 7.** Electrical resistivity tomography of the Cattle Lane site including a photograph and schematic of the site. Lateral homogeneity of the subsurface alluvium over at least 240 metres is indicated.

3210

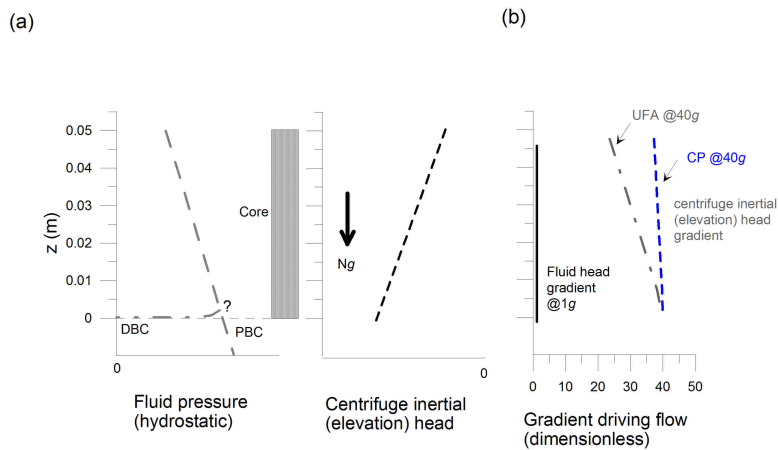


**Fig. 8. (a)** Conceptual relationship between hydrostatic fluid pressure, centrifuge inertial (elevation) head for a core in a centrifuge permeameter as a function of  $z$  (Fig. 1). The direction of centrifugal acceleration and fluid flow is indicated by the arrow  $N_g$ . Alternative drainage boundary condition (DBC) and pressure boundary condition (PBC) are indicated at the base of the core sample. **(b)** Fluid head gradient at  $1g$  and centrifuge inertial head gradients for the UFA and Broadbent (CP module) centrifuges at  $40g$ .

3211

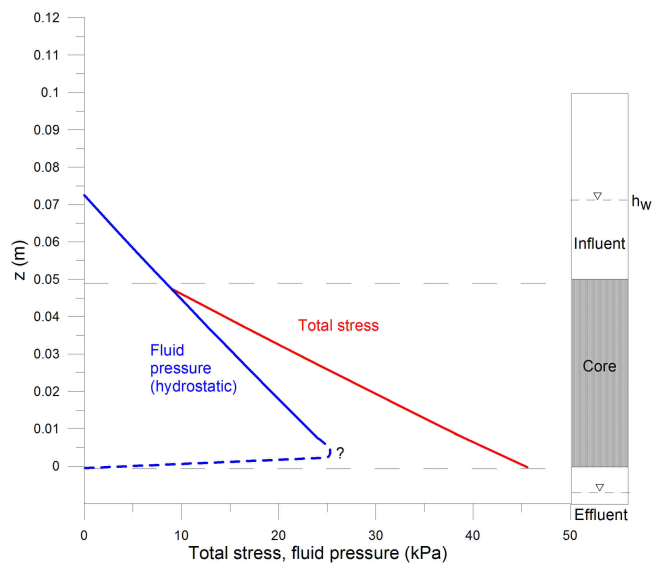


**Fig. 9.** Fluid head pressure (hydrostatic), total stress and effective stress (difference between total stress and effective stress) at  $40g$  in this study.

3212